Physica D ▮ (▮▮▮▮) ▮▮▮–▮▮▮

Contents lists available at ScienceDirect

Physica D

journal homepage: www.elsevier.com/locate/physd

Optical dispersive shock waves in defocusing colloidal media

X. An [a], T.R. Marchant [a,*], N.F. Smyth [a,b]

[a] School of Mathematics and Applied Statistics, University of Wollongong, Northfields Ave., Wollongong NSW 2522, Australia

[b] School of Mathematics, University of Edinburgh, James Clerk Maxwell Building, The King's Buildings, Peter Guthrie Tait Road, Edinburgh, Scotland, EH9 3FD, UK

HIGHLIGHTS

- Analysis of an optical dispersive shock wave in a defocusing colloidal medium.
- Powerful technique to derive leading and trailing edges of dispersive shock waves.
- Near perfect predictions for the properties of the dispersive shock wave.
- Useful model for comparisons with experimental work in colloidal media.

ARTICLE INFO

Article history:
Received 14 September 2016
Accepted 17 November 2016
Available online xxxx
Communicated by V.M. Perez-Garcia

Keywords:
Undular bores
Dispersive shock waves
Optical solitary waves
Modulation theory
Colloidal media

ABSTRACT

The propagation of an optical dispersive shock wave, generated from a jump discontinuity in light intensity, in a defocusing colloidal medium is analysed. The equations governing nonlinear light propagation in a colloidal medium consist of a nonlinear Schrödinger equation for the beam and an algebraic equation for the medium response. In the limit of low light intensity, these equations reduce to a perturbed higher order nonlinear Schrödinger equation. Solutions for the leading and trailing edges of the colloidal dispersive shock wave are found using modulation theory. This is done for both the perturbed nonlinear Schrödinger equation and the full colloid equations for arbitrary light intensity. These results are compared with numerical solutions of the colloid equations.

1. Introduction

Generic nonlinear wave equations, such as the Korteweg–de Vries (KdV), nonlinear Schrödinger (NLS) and Sine-Gordon equations, all possess hump-like travelling wave solutions, solitary waves [1], also referred to as solitons. However, the terms soliton and solitary wave are not strictly interchangeable, as a soliton is a solitary wave that has special properties. A solitary wave is a hump-like wave which decays to a constant level away from its peak [1]. To be termed a soliton a solitary wave must interact cleanly with other solitary waves, with the only evidence of their interaction being a possible phase change [1–3]. Another generic nonlinear wave structure is the undular bore, also called a dispersive shock wave (DSW) or collisionless shock wave [4]. The study of bores first arose in water wave theory [5,6]. Bores are the dispersive or dissipative resolution of an initial discontinuity in wave height, classic examples being the tidal bores which arise in coastal regions of strong tidal flow, such as the Severn Estuary in England and the Bay of Fundy in Canada, and the tsunamis generated by marine earthquakes and land slips. Bores in fluids fall into two broad categories, viscous bores and undular bores. As the name suggests, viscous bores are dominated by viscous loss and are steady wavetrains resulting from a balance between viscous loss, nonlinearity and dispersion [1,5,6]. Such bores with loss will not be of concern in the present work on optical DSWs. On the other hand, DSWs or undular bores arise when viscous effects are negligible and are unsteady wavetrains which spread continuously, with solitary waves at one edge and linear waves at the other. In the context of fluid flow, undular bores have been observed, studied and modelled in the atmosphere [7–9], on the continental shelf in the internal tide [10], in stratified fluids [11], in magma flow in geophysics [12–14], in Fermi gases [15] and Bose–Einstein condensates [16]. Of relevance to the present work, there have been experimental and theoretical studies of DSWs in nonlinear optical media such as photorefractive crystals [17–19], nonlinear optical fibres [20–22] and nonlinear thermal optical media [23,24]. While the terms DSW and undular bore refer to the same phenomenon and, in principle, are

* Corresponding author.
E-mail addresses: xa989@uowmail.edu.au (X. An), tim_marchant@uow.edu.au (T.R. Marchant), N.Smyth@ed.ac.uk (N.F. Smyth).

http://dx.doi.org/10.1016/j.physd.2016.11.004
0167-2789/

interchangeable, the first term will be used in the present work. This is because the term undular bore tends to be restricted to water wave theory and the term DSW is more commonly used for the phenomenon in other fields.

DSWs are unsteady wave forms and so finding solutions for them is not as straightforward as finding solutions for steady waves, such as solitary waves. It was not until the development of Whitham modulation theory [1,25,26] that a technique was developed which enabled the derivation of DSW solutions of suitable nonlinear wave equations. Whitham modulation theory is a method to analyse slowing varying periodic wavetrains using either a Lagrangian formulation of the equations or conservation equations [1], and is related to the method of multiple scales in asymptotic analysis. For this reason it is sometimes referred to as the method of averaged Lagrangians. It is also a nonlinear extension of the WKB method. The modulation equations derived using Whitham modulation theory are equations for the slowly varying parameters of the wavetrain, such as amplitude, wavenumber and mean height. If the underlying wavetrain is stable, then the modulation equations form a hyperbolic system and if it is unstable, the modulation equations form an elliptic system [1]. In particular, Whitham derived the modulation equations for the KdV equation, which were found to form a hyperbolic system [1,26]. It was subsequently realised that a simple wave (expansion fan) solution of these modulation equations was physically a DSW solution [27,28]. With this connection with Whitham modulation theory, DSW solutions could be derived for other nonlinear wave equations, such as the NLS equation [29], the Sine-Gordon equation [30] and the Gardner equation [31]. However, finding these DSW solutions as simple wave solutions relied on setting the hyperbolic modulation equations in Riemann invariant form, which is only guaranteed if the underlying nonlinear wave equation is integrable [32]. Recently, El [4,33,34] showed that, in general, hyperbolic modulation equations have a simplified structure at the leading and trailing edges of a DSW. This simplified structure was then exploited to determine its leading and trailing edges without a full knowledge of the Whitham modulation equations for the governing equation. For negative dispersion, the leading edge consists of solitary waves and the trailing edge linear waves, with the position of these waves swapped around for positive dispersion. This relaxation of the need for the full modulation equations then enabled the leading and trailing edges of DSWs governed by non-integrable equations to be determined [4,11,14,35,36]. In many observational measurements only the solitary wave edge of an DSW can be resolved [7–10,23,37], so the restriction of El's method to the leading and trailing edges of a DSW is less critical than may first appear.

In the present work the propagation of an optical DSW in the nonlinear optical medium of a colloidal suspension will be studied. The equations governing optical beam propagation in a colloid consist of an NLS-type equation for the beam coupled to an algebraic equation for the concentration of the colloid particles which depends on the beam intensity [38,39]. In the limit of low light intensity, these equations can be asymptotically reduced to a higher order NLS equation. While a colloid is normally a focusing medium, so that its refractive index increases with beam intensity, it can be made to be a defocusing medium [40,41], which then supports a DSW consisting of dark solitary waves at the trailing edge and linear waves at the leading edge [4,29,42]. The DSW is generated by a jump initial condition in optical beam intensity. While there have been previous studies of DSW in colloids [43,44], these have been for focusing colloids. In this case the waves of the DSW are modulationally unstable, so that the DSW structure has only a finite propagation length before becoming unstable. This is not the case for a defocusing colloidal medium. The leading and trailing edges of the colloid DSW are determined using El's method [4,33,34] based on both the full colloid equations and their limit in terms of a higher order NLS equation in the limit of low beam intensity. These modulation theory solutions are compared with full numerical solutions of the governing colloid equations. As well as determining the accuracy of modulation theory, these comparisons also determine the applicability of the low light intensity limit of the colloid equations.

2. Colloid equations

Let us consider the propagation of a polarised optical beam through a colloidal suspension. DSWs in nonlinear optical media are governed by NLS-type equations and, in the simplest approximation, are governed by $(1+1)$ dimensional equations [4,45]. Higher dimensional $(2+1)$ dimensional DSWs governed by NLS-type equations are much more difficult to analyse and need a non-trivial azimuthal vortex structure to be stable. Indeed, solutions of $(2+1)$ dimensional DSWs governed by not just NLS-type equations, but any nonlinear wave equation, are an open topic [46,47]. Hence, the optical beam generating the colloid DSW will be assumed to have a plane front. The z direction will then be taken to be the propagation direction, with the x direction orthogonal to this and the beam having no y dependence. The concentration of the colloid particles has a nonlinear dependence on the beam intensity. The colloid can be either a focusing medium, so that its refractive index increases with beam intensity [38,48], or defocusing, so that it decreases with intensity [40,41]. In order for a stable DSW to be generated, the colloidal medium will be assumed to be defocusing. Let us denote the concentration of the colloidal particles by η, with η_0 the constant background concentration in the absence of the optical beam. In the slowly varying, paraxial approximation the non-dimensional equations governing the propagation of the optical beam through the colloidal suspension are then [38,39]

$$i\frac{\partial u}{\partial z}+\frac{1}{2}\frac{\partial^2 u}{\partial x^2}-(\eta-\eta_0)u=0, \tag{1}$$

with the equation of state, that is the medium response equation,

$$|u|^2=g(\eta)-g_0,\quad g(\eta)=\frac{3-\eta}{(1-\eta)^3}+\ln\eta. \tag{2}$$

Here u is the complex valued envelope of the electric field of the optical beam and $g_0 = g(\eta_0)$. The Carnahan–Starling compressibility approximation has been used for the state relation g. Alternative models for the compressibility alter the form of g. The Carnahan–Starling approximation is valid up to the solid–fluid transition, which occurs at $\eta=\sqrt{2}\pi/9\approx 0.496$ in a hard-sphere fluid [49]. It should be noted that the nonlinear term in the NLS equation (1) for the optical beam has a negative coefficient, so that the equation is defocusing, in contrast to the focusing equation of previous work [38,39].

Hoefer [50] considered general properties of DSW solutions of generalised NLS equations of the form

$$i\frac{\partial u}{\partial z}+\frac{1}{2}\frac{\partial^2 u}{\partial x^2}-f(|u|^2)u=0, \tag{3}$$

with details determined for a power law nonlinearity f. While the colloid system (1) and (2) is in principle of this form, the nonlinearity f cannot be explicitly determined from the medium response equation (2). The colloid system then represents a further extension of the forms of nonlinear response in generalised NLS equations and the DSW solutions for such equations, in addition to the previously studied extension of a nonlocal response [35,51].

The simplest initial condition which will result in the generation of a DSW is a step initial condition in optical intensity,

$$u(x,0)=\begin{cases}u_-, & x<0,\\ u_+, & x>0.\end{cases} \tag{4}$$

Please cite this article in press as: X. An, et al., Optical dispersive shock waves in defocusing colloidal media, Physica D (2016), http://dx.doi.org/10.1016/j.physd.2016.11.004

We require that $u_- > u_+ \geq 0$ in order for the initial condition to be breaking so that a DSW is generated, in contrast to an expansion wave for $u_- < u_+$. The medium equation (2) then shows that the initial concentration of colloid particles is

$$\eta(x,0) = \begin{cases} \eta_-, & x < 0 \\ \eta_+, & x > 0, \end{cases} \tag{5}$$

where η_- is the concentration generated by the beam intensity u_- and η_+ by the intensity u_+. The intensity u and packing fraction are related by the state equation (2).

3. Low light intensity limit

The colloid equations (1) and (2) can be simplified in the limit in which the intensity $|u|^2$ of the light beam is low as the medium equation (2) can then be asymptotically solved for the concentration η in terms of $|u|^2$. Let us then set the concentration as

$$\eta = \eta_0 + \eta_1|u|^2 + \eta_2|u|^4 + \cdots. \tag{6}$$

The low intensity limit is equivalent to $|\eta - \eta_0| \ll 1$. The medium equation (2) can then be inverted to give

$$\eta - \eta_0 = \frac{|u|^2}{g'(\eta_0)} - \frac{g''(\eta_0)}{2g'(\eta_0)^3}|u|^4 + \cdots, \tag{7}$$

so that the electric field equation (1) becomes

$$i\frac{\partial u}{\partial z} + \frac{1}{2}\frac{\partial^2 u}{\partial x^2} - \left(g'(\eta_0)\right)^{-1}|u|^2 u + \frac{g''(\eta_0)}{2g'(\eta_0)^3}|u|^4 u = 0 \tag{8}$$

to second order in $|u|^2$. This is an NLS equation with a fifth order nonlinearity correction, which has been extensively studied [18,36,45]. It can be set in the standard form

$$i\frac{\partial u}{\partial z'} + \frac{1}{2}\frac{\partial^2 u}{\partial x'^2} - |u|^2 u + \alpha|u|^4 u = 0 \tag{9}$$

by using the rescaled variables

$$z = g'(\eta_0)z', \qquad x = \sqrt{g'(\eta_0)}x', \qquad \alpha = \frac{g''(\eta_0)}{2g'(\eta_0)^2}, \tag{10}$$

as the derivative $g'(\eta_0)$ of the constitutive law is positive.

The linear periodic wave solution of the higher order NLS equation (9) is

$$u = u_\infty e^{-i(u_\infty^2 - \alpha u_\infty^4)z'}. \tag{11}$$

Using this wave as the background carrier wave, we then find the grey solitary wave solution of the higher order NLS equation (9) as

$$u = \left[B\tanh C\theta + \frac{\alpha}{3}\left(B^3 + A^2 B\right)\tanh C\theta - \frac{\alpha}{3}B^3\tanh^3 C\theta + iA - i\frac{\alpha}{3}AB^2\tanh^2 C\theta\right]e^{-i(u_\infty^2 - \alpha u_\infty^4)z' + iVx'} + \cdots, \quad \text{where} \tag{12}$$

$$C = B - \alpha\left(B^3 + \frac{4}{3}A^2 B\right), \qquad A^2 + B^2 = u_\infty^2,$$

$$\theta = x' - \left[A + V - \alpha\left(\frac{2}{3}AB^2 + A^3\right)\right]z'.$$

V is velocity of the background level. In the limit $\alpha = 0$, the NLS grey soliton is obtained. This asymptotic solitary wave solution will be used in Section 6 to derive the amplitude of the leading solitary wave of the DSW in the limit of low light intensity.

Fig. 1 shows a typical DSW solution of the colloid equations (1) and (2). The parameters are $u_- = 1.0$, $u_+ = 0.5$ and $\eta_0 = 0.01$. Shown is a contour plot of the numerical simulation of

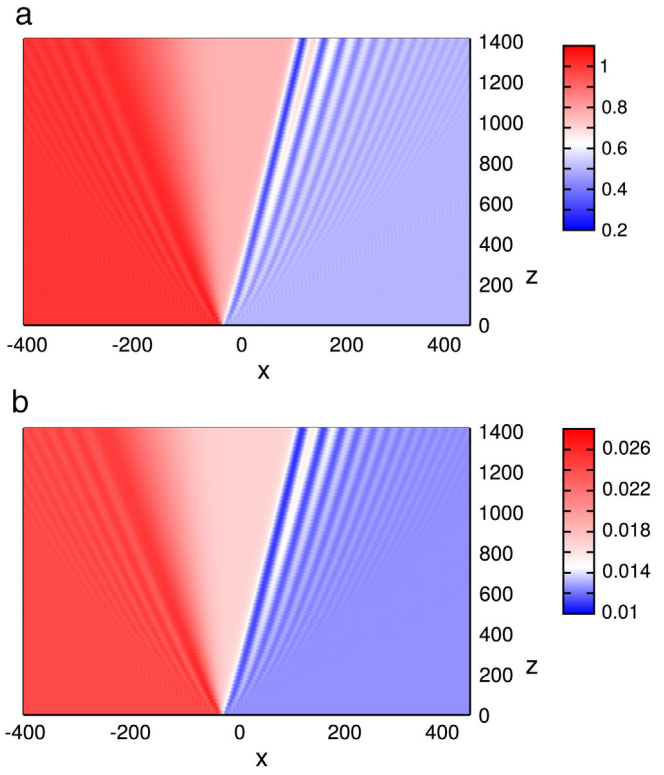

Fig. 1. DSW solution of the colloid equations (1) and (2). The parameters are $u_- = 1.0$, $u_+ = 0.5$ and $\eta_0 = 0.01$. Shown are contour plots of the numerical solution of (a) the electric field $|u|$ and (b) the packing fraction η.

(a) the electric field $|u|$ and (b) the packing fraction η. It can be seen that the solution consists of four sections. The first is the original levels u_+ and u_- ahead of and behind the DSW. The second is an intermediate shelf u_i behind the actual DSW with $u_+ < u_i < u_-$, with the third section a dispersionless level change linking the intermediate shelf u_i to the level behind u_-. It should be noted that there is a small amplitude wavetrain on the level u_-. This wavetrain is due to the smoothing of the discontinuity in derivative at the point the expansion wave links the level u_- [28]. The final, fourth, section is the actual DSW linking the intermediate shelf u_i to the level u_+ ahead. Each of these portions of the solution will be discussed in the following sections.

4. Dispersionless limit

As can be seen from Fig. 1, a DSW consists of two main wave forms, the DSW itself for which dispersion balances nonlinearity, and the region away from the DSW for which dispersion can be neglected [4,33,34]. To understand the solution in these two regions, it is simplest to set the colloid equations (1) and (2) in the so-called hydrodynamic form via the Madelung transformation

$$u = \sqrt{\rho}e^{i\phi}, \qquad v = \phi_x. \tag{13}$$

This transformation then sets the colloid equations in the form

$$\frac{\partial \rho}{\partial z} + \frac{\partial}{\partial x}(\rho v) = 0, \tag{14}$$

$$\frac{\partial v}{\partial z} + v\frac{\partial v}{\partial x} - \frac{\partial}{\partial x}\left(\frac{\rho_{xx}}{4\rho} - \frac{\rho_x^2}{8\rho^2}\right) + \frac{\partial \eta}{\partial x} = 0, \tag{15}$$

where

$$\rho = g(\eta) - g(\eta_0). \tag{16}$$

The system (14) and (15) is referred to as the hydrodynamic form as it is similar to the shallow water equations [1], with the first

Please cite this article in press as: X. An, et al., Optical dispersive shock waves in defocusing colloidal media, Physica D (2016), http://dx.doi.org/10.1016/j.physd.2016.11.004

of Eq. (14) that for mass conservation and the second (15) that for momentum conservation in this context. The initial condition is (4) and (5).

Away from the DSW, the solution is approximately non-dispersive as there are no significant waves, as seen from the typical solution displayed in Fig. 1. The non-dispersive limit of the hydrodynamic equations (14) and (15) is

$$\frac{\partial \rho}{\partial z}+\frac{\partial}{\partial x}(\rho v)=0, \qquad \frac{\partial v}{\partial z}+v\frac{\partial v}{\partial x}+\frac{1}{g'(\eta)}\frac{\partial \rho}{\partial x}=0, \qquad \frac{\partial \eta}{\partial x}=\frac{1}{g'(\eta)}\frac{\partial \rho}{\partial x}. \tag{17}$$

In Riemann invariant form, these equations are

$$v+\int_{\rho_+}^{\rho}\frac{d\rho}{\sqrt{\rho g'(\eta)}}=\text{constant}$$
$$\text{on } C_+ : \frac{dx}{dz}=V_+=v+\sqrt{\frac{\rho}{g'(\eta)}}, \tag{18}$$
$$v-\int_{\rho_+}^{\rho}\frac{d\rho}{\sqrt{\rho g'(\eta)}}=\text{constant}$$
$$\text{on } C_- : \frac{dx}{dz}=V_-=v-\sqrt{\frac{\rho}{g'(\eta)}}. \tag{19}$$

The dispersionless equations can be used to determine the level u_i of the intermediate shelf seen in Fig. 1. As noted above, the levels u_- and u_i are linked by an expansion wave, which is an expansion fan on the characteristic C_- with the Riemann invariant on C_+ constant in the fan. The intermediate shelf u_i terminates at the DSW, whose trailing edge has the velocity v_-. This simple wave solution is

$$\rho=\begin{cases}\rho_-, & \frac{x}{z}<-H_-,\\ \rho_f, & -H_-\le\frac{x}{z}\le M(\rho_-,\rho_i)-H_i,\\ \rho_i, & M(\rho_-,\rho_i)-H_i<\frac{x}{z}<v_-\end{cases} \tag{20}$$

and

$$v=\begin{cases}0, & \frac{x}{z}<-H_-,\\ M(\rho_-,\rho_f), & -H_-\le M(\rho_-,\rho_i)-H_i,\\ M(\rho_-,\rho_i), & M(\rho_-,\rho_i)-H_i<\frac{x}{z}<v_-.\end{cases} \tag{21}$$

The expressions for the edges of the expansion fan are involved and are

$$H_-=\sqrt{\frac{\rho_-}{g'(\eta_-)}}, \qquad M(\rho_-,\rho_i)=\int_{\rho_i}^{\rho_-}\frac{d\rho}{\sqrt{\rho g'(\eta)}},$$
$$H_i=\sqrt{\frac{\rho_i}{g'(\eta_i)}}, \qquad M(\rho_-,\rho_f)=\int_{\rho_f}^{\rho_-}\frac{d\rho}{\sqrt{\rho g'(\eta)}}. \tag{22}$$

The intensity $\rho=\rho_f$ on the expansion fan is the solution of

$$\rho_f=g'(\eta_f)\left[M(\rho_-,\rho_f)-\frac{x}{z}\right]^2. \tag{23}$$

This simple wave solution is not complete as the level $u_i=\sqrt{\rho_i}$ of the intermediate shelf is not yet determined. The intermediate level ρ_i is found by the requirement that the Riemann invariant along the characteristic C_- is constant through the DSW, which links the intermediate level to the level $u_+=\sqrt{\rho_+}$ ahead of the DSW [4,33,34]. Hence the wavenumber v on the intermediate shelf is

$$v_i=M(\rho_i,\rho_+). \tag{24}$$

Matching this value of v_i with the value given by the simple wave solution (21) finally gives that ρ_i is determined by the solution of

$$M(\rho_-,\rho_i)=M(\rho_i,\rho_+). \tag{25}$$

This completes the solution for the colloid DSW, except for the DSW itself.

In the low light intensity limit the Riemann invariant form (18) and (19) of the non-dispersive hydrodynamic equations can be approximated by

$$2\sqrt{\rho}-\frac{2}{3}\alpha\rho^{3/2}+v=\text{constant}$$
$$\text{on } C_+ : \frac{dx'}{dz'}=v+\sqrt{\rho}(1+\alpha\rho), \tag{26}$$
$$2\sqrt{\rho}-\frac{2}{3}\alpha\rho^{3/2}-v=\text{constant}$$
$$\text{on } C_- : \frac{dx'}{dz'}=v-\sqrt{\rho}(1+\alpha\rho). \tag{27}$$

The expansion fan solution (20) then becomes

$$\sqrt{\rho}=\begin{cases}u_-, & Q<\frac{x}{z},\\ \rho_{f_{hnls}}, & Q\le\frac{x}{z}\le G,\\ \sqrt{\rho_i}, & G<\frac{x}{z}<v_-,\end{cases} \tag{28}$$

with the limits of the expansion fan given by

$$Q=-\frac{u_-+\alpha u_-^3}{\sqrt{g'(\eta_0)}},$$
$$G=\frac{2u_--3\sqrt{\rho_i}-\frac{\alpha}{3}\left(2u_-^3+\rho_i^{3/2}\right)}{\sqrt{g'(\eta_0)}}. \tag{29}$$

The corresponding wavenumber v is determined by the intensity ρ given by (28) and is

$$v=2u_--2\sqrt{\rho}-\frac{2\alpha}{3}\left(u_-^3-\rho^{3/2}\right). \tag{30}$$

In the expansion fan the intensity $\rho=\rho_{f_{hnls}}$ is given by the solution of

$$3\sqrt{\rho_{f_{hnls}}}+\frac{1}{3}\alpha{\rho_{f_{hnls}}}^{3/2}=\left(2u_--\frac{2}{3}\alpha u_-^3\right)-\frac{x}{z}\frac{1}{\sqrt{g'(\eta_0)}}, \tag{31}$$

which completes the non-dispersion portion of the solution in the low light intensity limit.

In the same low intensity limit, Eq. (25) for the intermediate level ρ_i can be solved to give

$$\sqrt{\rho_i}=\frac{\sqrt{\rho_-}+\sqrt{\rho}_+}{2}+\frac{\alpha}{12}\left[\rho_-^{3/2}+\rho_+^{3/2}-\frac{1}{4}\left(\sqrt{\rho_-}+\sqrt{\rho_+}\right)^3\right]. \tag{32}$$

The wavenumber v_i on the intermediate shelf, given by (24), similarly becomes

$$v_i=\sqrt{\rho_-}-\sqrt{\rho_+}-\frac{\alpha}{12}\left[10\rho_-^{3/2}+2\rho_+^{3/2}-\frac{3}{2}\left(\sqrt{\rho_-}+\sqrt{\rho_+}\right)^3\right]. \tag{33}$$

This solution for the intermediate level is also needed for the determination of the leading and trailing edges of the DSW as the trailing edge of the DSW arises from this shelf, see Fig. 1.

Please cite this article in press as: X. An, et al., Optical dispersive shock waves in defocusing colloidal media, Physica D (2016), http://dx.doi.org/10.1016/j.physd.2016.11.004

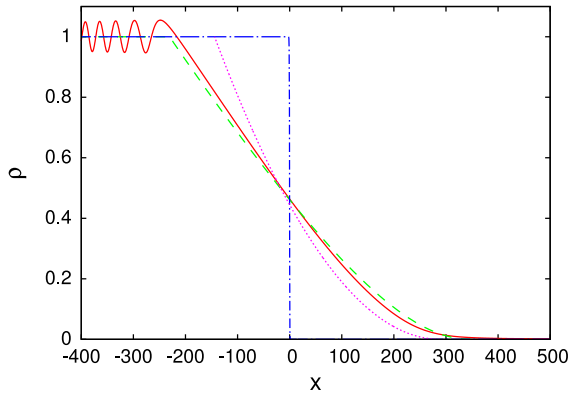

Fig. 2. The intensity ρ versus x at $z = 1500$. The parameters are $\rho_- = 1.0$, $\rho_+ = 0.0$ and $\eta_0 = 0.01$. Shown are the numerical solution of the colloid equations (1) and (2) for the initial jump condition (4) and the dam break solution (34) of colloid equation and (36) of the higher order NLS equation. Initial ρ: (dark blue) dot–dash line; numerical solution of colloid equation: (red) solid line; modulation solution of higher order NLS: pink (dotted) line; modulation solution of colloid equation: (green) dashed line. (For interpretation of the references to colour in this figure legend, the reader is referred to the web version of this article.)

5. Dam break solution

The simplest solution of the colloid equations (1) and (2) with the jump initial condition (4) is for $u_+ = 0$. In this limit, the intermediate shelf u_i disappears and there is only the expansion wave of the previous section linking the level u_- to $u_+ = 0$. The solution is then just the classical dam break solution of shallow water wave theory [1]. The expansion fan solution (20) and (21) then becomes

$$\rho = \begin{cases} \rho_-, & \dfrac{x}{z} < -H_-, \\ \rho_f, & -H_- \le M(\rho_-, 0), \\ 0, & \dfrac{x}{z} > M(\rho_-, 0) \end{cases} \tag{34}$$

and

$$v = \begin{cases} 0, & \dfrac{x}{z} < -H_-, \\ M(\rho_-, \rho_f), & -H_- \le \dfrac{x}{z} \le M(\rho_-, 0), \\ M(\rho_-, 0), & \dfrac{x}{z} > M(\rho_-, 0), \end{cases} \tag{35}$$

where, again, ρ_f is the solution of (23). As the intermediate shelf has disappeared, there is no DSW as no wavetrain is needed to bring the solution down from u_i to u_+.

In the low light intensity limit, this dam break solution becomes

$$\sqrt{\rho} = \begin{cases} u_-, & Q < \dfrac{x}{z}, \\ \rho_{f_{hnls}}, & Q \le \dfrac{x}{z} \le G_{dam}, \\ 0, & \dfrac{x}{z} > G_{dam}. \end{cases} \tag{36}$$

Here Q and G_{dam} are given by (29) and v is given by (30), with $\rho_i = 0$.

Fig. 2 shows the intensity ρ versus x at $z = 1500$. The parameters are $\rho_- = 1.0$, $\rho_+ = 0.0$ and $\eta_0 = 0.01$, so that the dam break solution applies. Compared are the numerical solution of the colloid equations (1) and (2) and the dam break solutions of the higher order NLS equation (28) and the colloid equation (34). It can be seen that there is excellent agreement between the numerical solution and the dam break solution of colloid equation, while the higher order NLS solution shows clear disagreement, indicating the importance of higher order terms in the colloid equations (1) and (2). The expansion fan itself lies in the region $-230 < x < 347$ as predicted by dam break solution the colloid equations and $-144 < x < 288$ by the dam break solution of the higher order NLS equation. The disagreement can be explained by the size of $|\alpha|$. As $\alpha = -0.425$, neglected terms of $\mathcal{O}(\alpha^2)$ and higher are important. It can be seen that there is a small amplitude dispersive wavetrain generated at the trailing edge of the expansion fan which is not accounted for by the present modulation theory. This wavetrain is due to the discontinuity in the derivative of the dam break solution at the trailing edge of the expansion fan and the flat level u_- behind the trailing edge. This small amplitude wavetrain is a general feature of expansion fan solutions in modulation theory and acts to smooth out this discontinuity [28].

6. Higher order NLS DSW

In general, when the level ahead u_+ is non-zero there is a DSW linking this level with an intermediate level of height u_i, as seen in Fig. 1. There is no known periodic wave solution of the colloid equations (1) and (2), and hence no basis to calculate the full Whitham modulation equations, from which the DSW solution could be determined. It is then convenient to use the method of El [4,33,34] to determine the leading and trailing edges of this DSW. This will be done in Section 7. However, due to the highly nonlinear constitutive relation (2), the exact solution of El's equations cannot be found and they have to be solved numerically. In this section, El's method will be used for the higher order NLS equation (9) as the leading and trailing edge equations can be solved exactly in this low intensity limit. It should be noted that El's method has been applied to similar higher order NLS equations in previous work [18,36]. The higher order NLS equation (8) differs from that used in this previous work only in the scaling of the cubic and quintic nonlinear terms due to the colloid constitutive relation (2). The present DSW solution for the leading and trailing edges for the higher order NLS equation (8) is then a rescaled version of that of this previous work.

El [4,33,34] showed that the leading and trailing edges of a DSW can be determined from the linear dispersion relation for the relevant equation. In hydrodynamic form the higher order NLS equation (9) is

$$\begin{aligned} &\frac{\partial \rho}{\partial z'} + \frac{\partial}{\partial x'}(\rho v) = 0, \\ &\frac{\partial v}{\partial z'} + v\frac{\partial v}{\partial x'} + (1 - 2\alpha\rho)\frac{\partial \rho}{\partial x'} - \frac{\partial}{\partial x'}\left(\frac{\rho_{x'x'}}{4\rho} - \frac{\rho_{x'}^2}{8\rho^2}\right) = 0. \end{aligned} \tag{37}$$

We then seek a linear travelling wave solution

$$\rho = \bar{\rho} + \rho_1 e^{i(kx' - \omega z')}, \qquad v = \bar{v} + v_1 e^{i(kx' - \omega z')}, \tag{38}$$

of these equations, where $|\rho_1| \ll \bar{\rho}$ and $|v_1| \ll |\bar{v}|$. This gives the dispersion relation

$$\begin{aligned} \omega &= \bar{v}k + k\sqrt{\bar{\rho}\,(1 - 2\alpha\bar{\rho}) + \frac{1}{4}k^2} \\ &= \bar{v}k + k\sqrt{\bar{\rho} + \frac{1}{4}k^2} - \alpha\bar{\rho}^2 k\left(\bar{\rho} + \frac{1}{4}k^2\right)^{-1/2} + \cdots. \end{aligned} \tag{39}$$

The determination of the leading and trailing edges of a DSW results from a matching of these edges with the dispersionless solution away from the DSW.

Please cite this article in press as: X. An, et al., Optical dispersive shock waves in defocusing colloidal media, Physica D (2016), http://dx.doi.org/10.1016/j.physd.2016.11.004

6.1. Linear wave edge of DSW

El [4,33,34] gives that the linear wave edge of the DSW, the leading edge, is determined by the differential equation

$$\frac{dk}{d\bar{\rho}} = \frac{\partial\omega}{\partial\bar{\rho}}\left(V_+ - \frac{\partial\omega}{\partial k}\right)^{-1}, \tag{40}$$

where V_+ is the velocity of the forward propagating characteristic (18). At the edges of the DSW, $\bar{v}$ and $\bar{\rho}$ are related due to the coincidence of two characteristics of the full modulation equations [4,33,34]. This relation is determined by the DSW jump condition which requires that the Riemann invariant on the C_- characteristic is the same at both ends of the DSW. This gives

$$\bar{v} = 2\sqrt{\bar{\rho}} - \frac{2}{3}\alpha\rho^{3/2} - 2\sqrt{\rho_+} + \frac{2}{3}\alpha\rho_+^{3/2}, \tag{41}$$

as $v = 0$ and $\rho = \rho_+$ ahead of the DSW.

Eq. (40) for the linear edge of the DSW can now be solved on using the dispersion relation (39) with $\bar{v}$ determined by (41). Substituting the dispersion relation (39) and the mean level (41) into the differential equation (40) gives

$$\frac{dk}{d\bar{\rho}} = \frac{1}{2}\frac{(1-4\alpha\bar{\rho})\,k}{\sqrt{\bar{\rho}}\,(1+\alpha\bar{\rho})\,W^{1/2} - W + \frac{k^2}{4}}, \tag{42}$$

where

$$W = \bar{\rho}\,(1-2\alpha\bar{\rho}) + \frac{k^2}{4}. \tag{43}$$

The change of variable

$$\gamma = \sqrt{1 + \frac{k^2}{4(\bar{\rho} - 2\alpha\bar{\rho}^2)}} \tag{44}$$

is now used to simplify this equation for the leading edge, so that it becomes

$$\frac{d\gamma}{d\bar{\rho}} = -\frac{1+\gamma}{2\bar{\rho}} + \alpha\left[\frac{4(1+\gamma)\gamma}{2\gamma+1} - (1+\gamma)\right]. \tag{45}$$

The leading, linear edge of the DSW can now be determined by solving this equation with the boundary condition which links it to the trailing, solitary wave edge. This boundary condition is $k = 0$ when $\bar{\rho} = \sqrt{\rho_i}$, with ρ_i given by (32), as a solitary wave has zero wavenumber [4,33,34]. It can then be found that

$$\gamma = 2\sqrt{\frac{\rho_i}{\bar{\rho}}} - 1 + \alpha\left[6\sqrt{\bar{\rho}\rho_i} + 32\rho_i - 38\frac{\rho_i^{3/2}}{\sqrt{\bar{\rho}}} + 128\frac{\rho_i^{3/2}}{\sqrt{\bar{\rho}}}\log\frac{4\sqrt{\rho_i} - \sqrt{\bar{\rho}}}{3\sqrt{\rho_i}}\right]. \tag{46}$$

The wavenumber k_+ at the leading, linear edge of the DSW is hence given by (44) and (46) with $\bar{\rho} = \rho_+$. Furthermore, the position of this edge of the DSW is given by the linear group velocity, which is

$$c_g = \frac{\partial\omega}{\partial k} = \frac{\rho_+ + \frac{1}{2}k_+^2}{\sqrt{\rho_+ + \frac{1}{4}k_+^2}} - \frac{\alpha\rho_+^3}{\left(\rho_+ + \frac{1}{4}k_+^2\right)^{3/2}}. \tag{47}$$

6.2. Solitary wave edge of DSW

The trailing, solitary wave, edge of the DSW can be determined in a similar fashion. This edge is determined in a similar fashion to the linear wave edge, but with a "conjugate" wavenumber $\tilde{k}$ and "conjugate" frequency $\tilde{\omega}$ related by the "conjugate" dispersion relation $\tilde{\omega} = -i\omega(i\tilde{k}, \bar{\rho}, \bar{v})$, where ω is given by the linear dispersion relation (39). Thus, the "conjugate" dispersion relation is

$$\tilde{\omega} = \bar{v}\tilde{k} + \tilde{k}\sqrt{\bar{\rho}\,(1-2\alpha\bar{\rho}) - \frac{1}{4}\tilde{k}^2} = \bar{v}\tilde{k} + \tilde{k}\sqrt{\bar{\rho} - \frac{1}{4}\tilde{k}^2} - \alpha\bar{\rho}^2\tilde{k}\left(\bar{\rho} - \frac{1}{4}\tilde{k}^2\right)^{-1/2} + \cdots. \tag{48}$$

As for the leading edge, the solitary wave edge of the DSW is determined by [4,33,34]

$$\frac{d\tilde{k}}{d\bar{\rho}} = \frac{\partial\tilde{\omega}}{\partial\bar{\rho}}\left(V_+ - \frac{\partial\tilde{\omega}}{\partial\tilde{k}}\right)^{-1}. \tag{49}$$

Again, the Riemann invariant condition (41) is used to relate $\bar{v}$ and $\bar{\rho}$ at the trailing edge of the DSW as, again, two of the modulation equations coincide at this edge. Using the conjugate dispersion relation (48) and the mean level (41), the trailing edge equation (49) becomes

$$\frac{d\tilde{k}}{d\bar{\rho}} = \frac{1}{2}\frac{(1-4\alpha\bar{\rho})\,\tilde{k}}{\sqrt{\bar{\rho}}\,(1+\alpha\bar{\rho})\,V^{1/2} - V + \frac{\tilde{k}^2}{4}}, \tag{50}$$

with

$$V = \bar{\rho}\,(1-2\alpha\bar{\rho}) - \frac{\tilde{k}^2}{4}. \tag{51}$$

Again, the change of variable

$$\tilde{\gamma} = \sqrt{1 - \frac{\tilde{k}^2}{4(\bar{\rho} - 2\alpha\bar{\rho}^2)}} \tag{52}$$

is now used to simplify this equation, which becomes

$$\frac{d\tilde{\gamma}}{d\bar{\rho}} = -\frac{1+\tilde{\gamma}}{2\bar{\rho}} + \alpha\left[\frac{4(1+\tilde{\gamma})\tilde{\gamma}}{2\tilde{\gamma}+1} - (1+\tilde{\gamma})\right]. \tag{53}$$

This equation is solved with the boundary condition linking the trailing edge with the linear, leading edge of the DSW, so that $\tilde{k} = 0$ at $\bar{\rho} = \rho_+$ [4,33,34]. The trailing edge solution is then found to be

$$\tilde{\gamma} = 2\sqrt{\frac{\rho_+}{\bar{\rho}}} - 1 + \alpha\left(6\sqrt{\bar{\rho}\rho_+} + 32\rho_+ - 38\frac{\rho_+^{3/2}}{\sqrt{\bar{\rho}}} + 128\frac{\rho_+^{3/2}}{\sqrt{\bar{\rho}}}\log\frac{4\sqrt{\rho_+} - \sqrt{\bar{\rho}}}{3\sqrt{\rho_+}}\right). \tag{54}$$

The conjugate wavenumber $\tilde{k}_i$ at the trailing edge of the DSW is finally given by (54) and (52) with $\bar{\rho} = \rho_i$ and ρ_i given by (32).

The position of the trailing, solitary wave, edge of the DSW is determined by the solitary wave velocity

$$v_- = \frac{\tilde{\omega}}{\tilde{k}} = v_i + \sqrt{\rho_i - \frac{1}{4}\tilde{k}_i^2} - \frac{\alpha\rho_i^2}{\sqrt{\rho_i - \frac{1}{4}\tilde{k}_i^2}}. \tag{55}$$

Finally, the amplitude of the trailing edge solitary wave of the DSW can be deduced from the grey solitary wave solution (12). Let us define the amplitude of the trailing edge solitary wave as

$$A_s = u_i - A, \tag{56}$$

which is the difference between the intermediate level u_i and the minimum of the solitary wave $|u|$. The velocity (12) of the (grey) solitary wave is given by the amplitude/velocity relation

$$v_- = A + v_i - \alpha\left(\frac{2}{3}AB^2 + A^3\right). \tag{57}$$

Please cite this article in press as: X. An, et al., Optical dispersive shock waves in defocusing colloidal media, Physica D (2016), http://dx.doi.org/10.1016/j.physd.2016.11.004

On noting that $A^2 + B^2 = u_i^2$ and $|\alpha| \ll 1$, this equation can be solved to give

$$A = v_- - v_i + \frac{1}{3}\alpha(v_- - v_i)\left[2u_i^2 + (v_- - v_i)^2\right]. \tag{58}$$

This amplitude expression is similar to the equivalent results (92) in [18] and (66) in [36]. The difference between these expressions and the present ones is that the present results are derived based on the general grey soliton solution (12) of the higher order NLS equation for the colloid response (2). It should be noted that the leading and trailing edge velocities (47) and (55), respectively, are in the scaled (x', z') coordinates and need to be transformed back to the coordinates (x, z) via the transformations (10) to be compatible with the colloid equations (1) and (2).

7. Full colloid DSW

In the previous section the leading and trailing edges of the DSW solution of the higher order NLS equation (8) were determined by using the theory of El [4,33,34], which is an asymptotic approximation to the edges of the DSW of the full colloid equations (1) and (2) in the limit of low light intensity. This leads to explicit solutions for the leading and trailing edges, detailed in Sections 6.1 and 6.2. The same method will now be used to determine the leading and trailing edges of the DSW solution of the full colloid equations (1) and (2). However, due to the complexity of the medium Eq. (2) the differential equations for the leading and trailing edges cannot be solved explicitly and need to be solved numerically.

The dispersion relation for the full colloid equations can be found by substituting the linear wave solution

$$\rho = \bar\rho + \rho_1 e^{i(kx-\omega z)}, \qquad v = \bar v + v_1 e^{i(kx-\omega z)}, \tag{59}$$

where $|\rho_1| \ll \bar\rho$ and $|v_1| \ll |\bar v|$, into the hydrodynamic equation (15). This gives

$$\omega = k\bar v + k\sqrt{\frac{\bar\rho}{g'(\bar\eta)} + \frac{1}{4}k^2}, \qquad \text{with } g(\bar\eta) - g_0 = \bar\rho. \tag{60}$$

Again, at the trailing and leading edges of the DSW $\bar v$ is related to $\bar\rho$ through the condition that the Riemann invariant on the characteristic C_- (19) is the same at the two edges of the DSW. We then have

$$\bar v = \int_{\rho_+}^{\bar\rho} \frac{d\rho}{\sqrt{\rho g'(\eta)}}. \tag{61}$$

7.1. Linear wave edge of DSW

The leading, linear wave, and trailing, solitary wave, edges of the DSW solution of the full colloid equations (1) and (2) can be determined in a similar fashion as was done in Section 6 for the DSW solution the higher order NLS equation (8).

The leading, linear wave, edge of the DSW is determined by the differential equation (40). On using the full dispersion relation (60) and expression (61) for $\bar v$, this equation becomes

$$\frac{dk}{d\bar\rho} = \frac{\frac{k}{\sqrt{\bar\rho g'(\bar\eta)}}\sqrt{\frac{\bar\rho}{g'(\bar\eta)} + \frac{1}{4}k^2} + \frac{1}{2}k\left(\frac{1}{g'(\bar\eta)} - \frac{\bar\rho g''(\bar\eta)}{g'^3(\bar\eta)}\right)}{\sqrt{\frac{\bar\rho}{g'(\bar\rho)}}\sqrt{\frac{\bar\rho}{g'(\bar\eta)} + \frac{1}{4}k^2} - \frac{\bar\rho}{g'(\bar\eta)} - \frac{1}{2}k^2}. \tag{62}$$

As for the higher order NLS DSW of Section 6 this equation is simplified using the change of variable

$$\gamma(\bar\rho) = \sqrt{1 + \frac{1}{4}\frac{k^2 g'(\bar\eta)}{\bar\rho}}. \tag{63}$$

The leading, linear edge of the DSW is then determined by

$$\frac{d\gamma}{d\bar\rho} = -\frac{(1+\gamma)\left(\frac{2}{g'(\bar\eta)} + (2\gamma-1)\left(\frac{\bar\rho}{g'(\bar\eta)}\right)'\right)}{2(2\gamma+1)\left(\frac{\bar\rho}{g'(\bar\eta)}\right)}. \tag{64}$$

This equation is solved with the condition $k(\rho_i) = 0$ which connects the linear edge of the DSW to the solitary wave edge [4,33,34], so that $\gamma(\rho_i) = 1$. With this solution the wavenumber at the leading edge of the DSW is

$$k = k(\rho_+) = 2\sqrt{\frac{\rho_+}{g'(\eta_+)}}\sqrt{\gamma^2(\rho_+) - 1}. \tag{65}$$

The position of the leading edge of the DSW is therefore finally given by the group velocity

$$c_g = \frac{\partial\omega}{\partial k} = \sqrt{\frac{\rho_+}{g'(\eta_+)}}\left(2\gamma(\rho_+) - \frac{1}{\gamma(\rho_+)}\right). \tag{66}$$

This leading edge position will be compared with numerical solutions of the colloid equations (1) and (2) in Section 9.

7.2. Solitary wave edge of DSW

The trailing, solitary wave, edge of the bore is determined in a similar fashion. The equation governing the trailing edge of the DSW is (49). As for the higher order NLS equation DSW, in general the "conjugate" dispersion relation is given by $\tilde\omega = -i\omega(i\tilde k, \bar\rho, \bar v)$, so that the linear dispersion relation (60) gives for the colloid DSW

$$\tilde\omega = \tilde k\bar v + \tilde k\sqrt{\frac{\bar\rho}{g'(\bar\eta)} - \frac{1}{4}\tilde k^2}, \quad \text{with } g(\bar\eta) - g_0 = \bar\rho. \tag{67}$$

With these conjugate variables and the relation (61) between $\bar v$ and $\bar\rho$ at the trailing edge of the DSW, Eq. (49) gives that the trailing edge is determined by

$$\frac{d\tilde k}{d\bar\rho} = \frac{\frac{\tilde k}{\sqrt{\bar\rho g'(\bar\eta)}}\sqrt{\frac{\bar\rho}{g'(\bar\eta)} - \frac{1}{4}\tilde k^2} + \frac{1}{2}\tilde k\left(\frac{1}{g'(\bar\eta)} - \frac{\bar\rho g''(\bar\eta)}{g'^3(\bar\eta)}\right)}{\sqrt{\frac{\bar\rho}{g'(\bar\rho)}}\sqrt{\frac{\bar\rho}{g'(\bar\eta)} - \frac{1}{4}\tilde k^2} - \frac{\bar\rho}{g'(\bar\eta)} + \frac{1}{2}\tilde k^2}. \tag{68}$$

As for the linear edge, this equation can be simplified by the change of variable

$$\tilde\gamma(\bar\rho) = \sqrt{1 - \frac{1}{4}\frac{\tilde k^2 g'(\bar\eta)}{\bar\rho}}, \tag{69}$$

so that the final equation for the trailing, solitary wave edge is

$$\frac{d\tilde\gamma}{d\bar\rho} = -\frac{(1+\tilde\gamma)\left(\frac{2}{g'(\bar\eta)} + (2\tilde\gamma-1)\left(\frac{\bar\rho}{g'(\bar\eta)}\right)'\right)}{2(2\tilde\gamma+1)\left(\frac{\bar\rho}{g'(\bar\eta)}\right)}. \tag{70}$$

This equation is solved with the condition $\tilde k(\rho_+) = 0$ [4,33,34] which connects the trailing edge to the leading edge, giving $\tilde\gamma(\rho_+) = 1$. With this solution, the velocity of the trailing edge of the DSW is

$$v_- = \frac{\tilde\omega}{\tilde k} = \int_{\rho_+}^{\rho_i} \frac{d\rho}{\rho\sqrt{g'(\eta)}} + \tilde\gamma(\rho_i)\sqrt{\frac{\rho_i}{g'(\eta_i)}}, \tag{71}$$

on using expression (61) for $\bar v$.

The differential equations (64) and (70) for the leading and trailing edges of the DSW, respectively, were solved numerically. The solution for the trailing edge of the DSW is not complete yet as, while (71) gives the velocity of the trailing edge, the amplitude of

Please cite this article in press as: X. An, et al., Optical dispersive shock waves in defocusing colloidal media, Physica D (2016), http://dx.doi.org/10.1016/j.physd.2016.11.004

the solitary wave at the trailing edge has not been determined. The colloid equations (1) and (2) have no known exact solitary wave solutions. However, the exact amplitude–velocity relation for the grey colloid solitary wave can be found without knowledge of this solution as (see Appendix)

$$V_s = \frac{\sqrt{2}|f_m|\sqrt{\sigma u_\infty^2 - \sigma|f_m|^2 + F(\eta_m, \eta_\infty)}}{u_\infty^2 - |f_m|^2}, \tag{72}$$

with $|f_m|$ the minimum value of $|u|$ and u_∞ the background carrier wave amplitude. The amplitude of the grey solitary wave is then

$$A_s = u_\infty - |f_m|, \tag{73}$$

the difference between the background level u_∞ and the minimum of $|u|$. We now recognise V_s as the difference between leading solitary wave velocity v_- from (71) and v_i from (24). The minimum $|f_m|$ is found by applying Newton's method to (72), resulting in the amplitude A_s. Hoefer [50] obtained general results for DSW solutions for NLS equations with a general nonlinearity $f(|u|^2)u$. The electric field equation (1) has a nonlinearity of this form, but without an explicit expression for f as the nonlinearity $(\eta - \eta_0)u$ is determined implicitly from the medium response (2). Hoefer found that in this general case the structure of the simple wave solution of the Whitham modulation equations for the DSW can break down in that the characteristic velocity of the simple wave ceases to be monotonic, which results in the formation of a multi-phase wavetrain [1,4,14]. In terms of the present work, this can occur if

$$V_+ = \frac{\partial\omega}{\partial k} \quad \text{or} \quad V_+ = \frac{\partial\tilde{\omega}}{\partial\tilde{k}} \tag{74}$$

in Eqs. (40) and (49) for the leading and trailing edges of the DSW. It can be seen from the specific Eqs. (64) and (70) for the leading and trailing edges that such a breakdown of the simple wave solution cannot occur for the colloid equations.

8. Vacuum point

As the jump height $u_i - u_+$ increases, the amplitudes of the waves in the DSW grow until there is a jump height for which the trailing solitary wave of the DSW has its minimum at $|u| = |f_m| = 0$. This point is referred to as the vacuum point [29]. At the vacuum point the trailing grey solitary wave of the DSW becomes dark as $|f_m| = 0$ and the amplitude–velocity (72) gives $V_s = 0$. Hence, the velocity of the trailing edge of the DSW is $v_- = v_i$ and the trailing edge conjugate dispersion relation (67) gives

$$\frac{\rho_i}{g'(\eta_i)} = \frac{1}{4}\tilde{k}^2. \tag{75}$$

This condition cannot be solved exactly to determine the vacuum point. However, it can be solved from expression (69) for the conjugate wavenumber $\tilde{k}$, with $\tilde{\gamma}$ determined by numerically solving the trailing edge equation (70).

The vacuum point condition (75) can be asymptotically solved in the low power limit. The higher order NLS equation conjugate dispersion relation (48) gives the onset of the vacuum point as

$$\rho_i - 2\alpha\rho_i^2 = \frac{1}{4}\tilde{k}^2. \tag{76}$$

Using the conjugate wavenumber $\tilde{k}$ determined by (52) and (54), the vacuum point then first occurs when ρ_+ and ρ_i satisfy

$$2\sqrt{\frac{\rho_+}{\rho_i}} + \alpha\left(6\sqrt{\rho_i\rho_+} + 32\rho_+ - 38\frac{\rho_+^{3/2}}{\sqrt{\rho}} + 128\frac{\rho_+^{3/2}}{\sqrt{\rho_i}}\log\frac{4\sqrt{\rho_+} - \sqrt{\rho_i}}{3\sqrt{\rho_+}}\right) = 1. \tag{77}$$

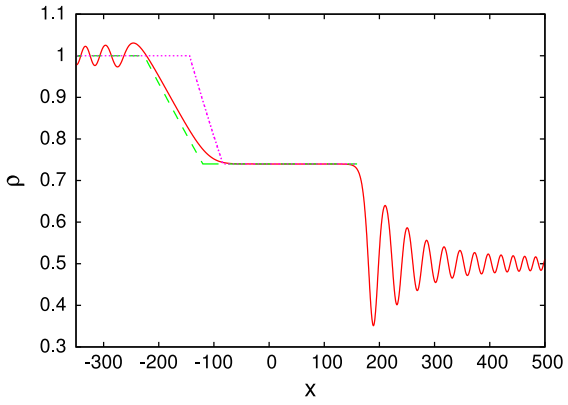

Fig. 3. The intensity ρ versus x at $z = 1500$. The parameter values are $\rho_- = 1.0$, $\rho_+ = 0.5$ and $\eta_0 = 0.01$. Shown are the numerical solution of the colloid equations (1) and (2) for the initial condition (4), the solution (20) and (25) of the non-dispersive colloid equations and non-dispersive solution (28) of the higher order NLS equation. Numerical solution: red (solid) line; solution of the higher order NLS equation: pink (dotted) line; solution of the colloid equation: green (dashed) line. (For interpretation of the references to colour in this figure legend, the reader is referred to the web version of this article.)

9. Comparison with numerical solutions

In this section, numerical solutions of the colloid equations (1) and (2) with the jump initial condition (4) will be compared with the modulation solutions of the NLS equation (higher order NLS equation with $\alpha = 0$), the higher order NLS equation and the full colloid equations. The numerical solutions of the colloid equations (1) and (2) were obtained using the numerical scheme of [43]. The electric field Eq. (1) was solved using a hybrid method with central differences used to approximate the spatial derivatives and the 4th order Runge–Kutta scheme used to propagate forward in the time-like variable z. The algebraic constitutive law (2) was solved using Newton's method. The full numerical scheme was found to be stable and has error $O(\Delta z^4, \Delta x^2)$ for discretisation Δz and Δx.

Fig. 3 shows the optical intensity ρ versus x at $z = 1500$. The parameter values are $\rho_- = 1.0$, $\rho_+ = 0.5$ and $\eta_0 = 0.01$. Compared are the non-dispersive modulation solution of the colloid equations (1) and (2) and the higher order NLS equation (8), as well as the numerical solution of the colloid equations. The expansion fan lies in the region $-227 < x \le -120$ as predicted by the modulation solution of the colloid equation and $-144 < x \le -84$ by the modulation solution of the higher order NLS equation. Also, the intermediate level lies in $-120 \le x < 160$ as given by the modulation solution of the colloid equations and $-84 \le x < 155$ as given by the higher order NLS equation modulation solution. As for the dam break solution, there is again excellent agreement between the modulation theory solution (20) and the numerical solution, but the higher order NLS solution (28) shows significant differences due to higher order terms being important. There is again a backward propagating small amplitude wavetrain on the initial level ρ_-, which is again generated by the smoothing due to dispersion of the discontinuity in slope of the modulation simple wave solution where it joins the level ρ_-. As $\rho_+ \neq 0$, a DSW is generated ahead of the intermediate level ρ_i.

Fig. 4 shows the intermediate level ρ_i versus ρ_+. The parameter values are $\rho_- = 1.0$ and $\eta_0 = 0.01$. Shown are numerical solutions and the full modulation solution (25) of the colloid equations (1) and (2), the higher NLS equation modulation theory solution (32) and the NLS equation modulation theory solution (32) with $\alpha = 0$. It can be seen that both the full non-dispersive solution and the higher order NLS equation solution are in excellent agreement with the full numerical solution. As $\rho_+ \to 1$, all the modulation theory solutions converge to $\rho_i = 1$ as in this limit there is no initial jump and the full solution is $\rho = 1$. As ρ_+

Please cite this article in press as: X. An, et al., Optical dispersive shock waves in defocusing colloidal media, Physica D (2016), http://dx.doi.org/10.1016/j.physd.2016.11.004

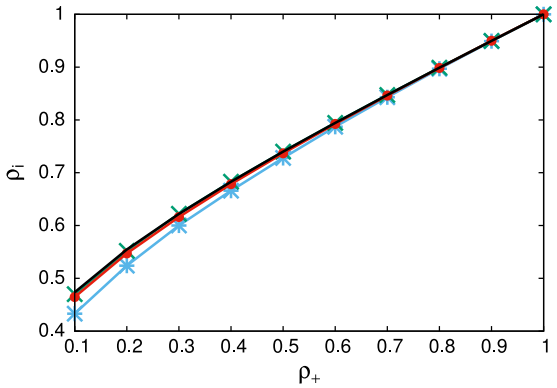

Fig. 4. The intermediate level ρ_i versus ρ_+. The parameter values are $\rho_- = 1.0$ and $\eta_0 = 0.01$. Shown are the NLS equation modulation solution (32) with $\alpha = 0$: (light blue) line with ⋆; higher order NLS equation modulation solution (32): (red) line with •; modulation solution of full colloid equation (25): (green) line with ×; numerical solution of colloid equations: (black) line. (For interpretation of the references to colour in this figure legend, the reader is referred to the web version of this article.)

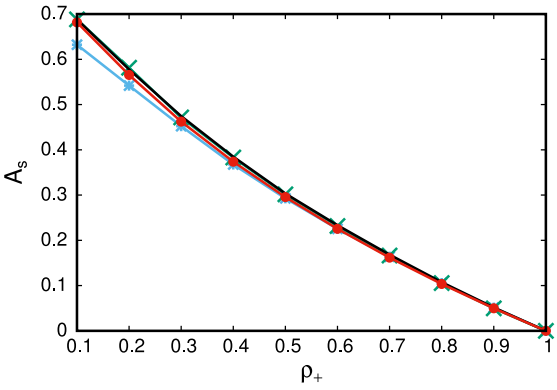

Fig. 5. The trailing solitary wave amplitude A_s versus ρ_+. The parameter values are $\rho_- = 1.0$ and $\eta_0 = 0.01$. Shown are the full numerical solution of the colloid equations (1) and (2) and modulation theory. NLS modulation theory (56) with $\alpha = 0$: (light blue) line with ⋆; higher order NLS modulation theory (56): (red) line with •; full modulation theory (73): (green) line with ×; numerical solution: black line. (For interpretation of the references to colour in this figure legend, the reader is referred to the web version of this article.)

decreases, the intermediate level decreases from the level behind and the differences between the modulation theory and numerical solutions increase. It should be noted that a vacuum point arises for $\rho_+ < 0.1$ and the modulation theory solutions are not valid below this level. Unfortunately, to continue the modulation theory solution below the vacuum point requires a knowledge of the full modulation equations [29]. It is important to note that the intermediate level as given by modulation theory for the NLS equation is in excellent agreement with the numerical values, except in the limit of large jumps $\rho_- - \rho_+$ towards the vacuum point, with the maximum error 8.5%. Higher order NLS equation modulation theory gives values for the intermediate level ρ_i which are almost identical with those of full modulation theory and with numerical results, which is expected given the accurate predictions of NLS equation modulation theory. Modulation theory for the higher order NLS equation gives intermediate levels which differ by at most 2.8% from numerical values.

Fig. 5 shows the amplitude A_s of the trailing solitary wave versus ρ_+. The parameter values are $\rho_- = 1.0$ and $\eta_0 = 0.01$. Shown are the numerical solution and the modulation theory amplitude (73) for the full colloid equations, the amplitude (56) for the higher order NLS equation and the amplitude (56) for the NLS equation (when $\alpha = 0$). It can be seen that the full modulation

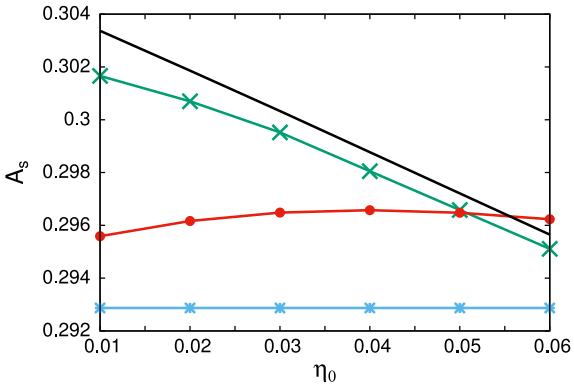

Fig. 6. The trailing solitary wave amplitude A_s versus the background packing fraction η_0. The parameter values are $\rho_- = 1.0$ and $\rho_+ = 0.5$. Shown are full numerical solutions of the colloid equations (1) and (2) and modulation theory. NLS equation modulation theory (56) with $\alpha = 0$: (light blue) line with ⋆; higher order NLS equation modulation theory (56): (red) line with •; full modulation theory (73): (green) line with ×; numerical solution: (black) line. (For interpretation of the references to colour in this figure legend, the reader is referred to the web version of this article.)

theory gives amplitudes in excellent agreement with numerical solutions for the full range of jump heights $\rho_- - \rho_+$. As for the intermediate level both full modulation theory and modulation theory for the higher order NLS equation give amplitudes in near perfect agreement with numerical results. The full colloid equation modulation amplitude differs by at most 0.5% and the higher order NLS equation modulation amplitude differs by at most 2% from the numerical values. Again, as for the intermediate level, modulation theory for the NLS equation gives amplitudes in good agreement with numerical solutions, except for large jump heights with ρ_+ near the vacuum point, at which point the modulation amplitude differs by 7% from the numerical value. The numerical and modulation amplitudes converge to $A_s = 0$ as $\rho_+ \to 1$ as the jump vanishes in this limit.

Fig. 6 shows the amplitude A_s of the trailing solitary wave of the DSW versus the background packing fraction η_0. The parameter values are $\rho_- = 1.0$ and $\rho_+ = 0.5$. Shown are amplitudes from numerical solutions of the colloid equations (1) and (2), the full modulation theory amplitude (73), the NLS equation modulation theory amplitude (56) with $\alpha = 0$ and the higher order NLS equation amplitude (56). The full modulation theory is, again, in excellent agreement with the numerical results, with an overall difference less than 0.5%. In contrast to the comparisons of Figs. 4 and 5, the amplitudes as given by the modulation theories for the NLS and higher order NLS equations show significant differences from the numerical values. For high background packing fractions the full modulation theory and the NLS and higher order NLS equation modulation theories give similar results, but the NLS and higher order NLS modulation theories show significant disagreement with the numerical results as the background packing fraction decreases. The NLS and higher order NLS equation modulation theories differ by 2.9% and 2.0% from numerical results in this limit.

Fig. 7 shows the trailing solitary wave velocity v_- versus ρ_+. The parameter values are $\rho_- = 1.0$ and $\eta_0 = 0.01$. Compared are the numerical velocity of the trailing solitary wave of the DSW and the modulation theory values, the full modulation theory value (71), the higher order NLS modulation theory value (55) and the NLS modulation theory value (55) with $\alpha = 0$. These comparisons are shown down to $\rho_+ = 0.1$, at which value the vacuum point first appears and the modulation theories of Sections 6 and 7 cease to be valid. As for the previous comparisons, the full modulation theory velocity is in excellent agreement with the numerical velocity, with a difference less of than 0.3%. The higher order NLS

Please cite this article in press as: X. An, et al., Optical dispersive shock waves in defocusing colloidal media, Physica D (2016), http://dx.doi.org/10.1016/j.physd.2016.11.004

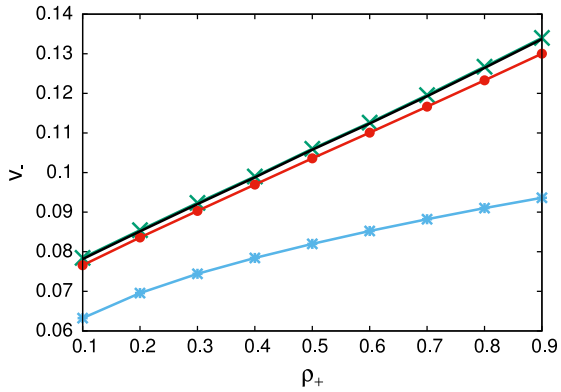

Fig. 7. The trailing solitary wave velocity v_- versus ρ_+. The parameter values are $\rho_- = 1.0$ and $\eta_0 = 0.01$. Shown are: NLS modulation theory (55) with $\alpha = 0$: (light blue) line with ⋆; higher order NLS modulation theory (55): (red) line with •; full modulation theory (71): (green) line with ×; numerical solution of colloid equations (1) and (2): (black) line. (For interpretation of the references to colour in this figure legend, the reader is referred to the web version of this article.)

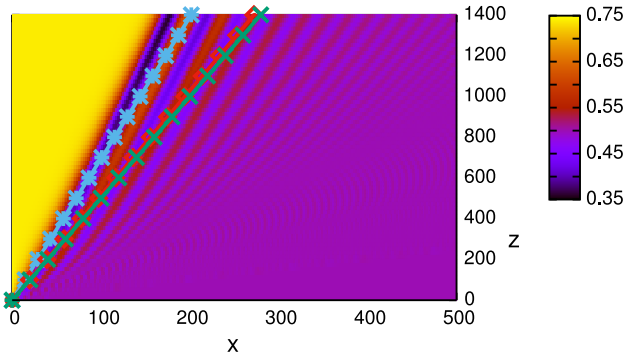

Fig. 8. Contour plot of the DSW portion of the numerical solution of the colloid equations (1) and (2). Superimposed are the positions of the leading, linear edge of the DSW as given by the group velocity c_g of modulation theory. The parameter values are $\rho_- = 1.0$, $\rho_+ = 0.5$, and $\eta_0 = 0.01$. NLS modulation theory (47) with $\alpha = 0$: (light blue) line with ⋆; higher order NLS modulation theory (47): (red) line with ◇; full modulation theory (66): (green) line with ×. (For interpretation of the references to colour in this figure legend, the reader is referred to the web version of this article.)

equation modulation theory gives a velocity in good agreement with the numerical value, but showing differences from it, unlike the intermediate level and amplitude comparisons of Figs. 4 and 5. As for the amplitude comparison of Fig. 6 modulation theory for the NLS equation does not yield a good prediction for the trailing solitary wave velocity, with differences ranging from 19% to 30%, showing the importance of higher order effects in determining the trailing solitary wave velocity.

Fig. 8 shows a contour plot of the DSW portion of a numerical solution of the colloid equations (1) and (2). To investigate the accuracy of the modulation theory prediction of the leading edge of the DSW by the linear group velocity c_g, this figure also has superimposed the leading edge prediction of the modulation theories of Sections 6.1 and 7.1. The parameter values used are $\rho_- = 1.0$, $\rho_+ = 0.5$ and $\eta_0 = 0.01$. The full modulation theory front position is given by the group velocity (66) and the higher order NLS equation modulation theory front position is given by the group velocity (47). The front position as given by the NLS equation modulation theory is the higher order NLS result (47) with $\alpha = 0$. This comparison is more complicated than the similar comparison of the trailing, solitary wave edge of Fig. 7 as numerical solutions show no distinct leading edge, in contrast to the predictions of modulation theory, with an extended train of waves of decreasing amplitude bringing the level back to

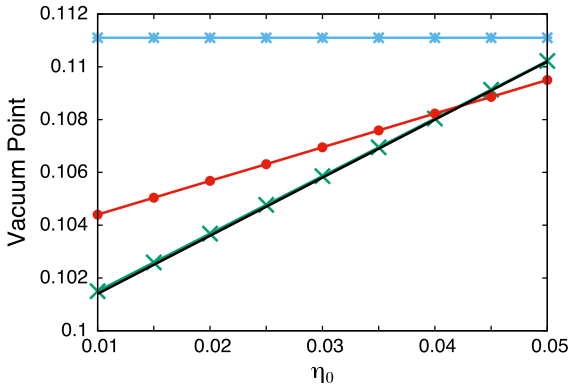

Fig. 9. Vacuum point versus background packing fraction η_0 for $\rho_- = 1.0$. Shown are the NLS modulation theory prediction (77) with $\alpha = 0$: (light blue) line with ⋆; higher order NLS modulation theory prediction (77): (red) line with •; full modulation theory prediction (75): (green) line with ×; numerical solution of colloid equations (1) and (2): (black) line. (For interpretation of the references to colour in this figure legend, the reader is referred to the web version of this article.)

ρ_+ [4,28]. Nevertheless, the front position comparison of Fig. 8 shows that the full modulation theory gives a front position which encompasses the majority of the larger amplitude waves of the DSW. As for the trailing edge comparison of Fig. 7, the higher order NLS equation modulation theory gives a good approximation to the leading edge position, while NLS equation modulation theory is not in agreement with numerical solutions. This again indicates that the higher order terms in the constitutive law (2) are important and that the response of the medium to the optical beam cannot be approximated by Kerr's Law. It should be noted for the comparisons of Fig. 8 that, in general, modulation theory does not do as well in predicting the linear edge position of a DSW than the solitary wave edge [4,28,52–54]. In terms of asymptotic theory there is an additional layer of linear waves between the initial level and the linear edge of the Whitham modulation theory solution [52–54].

Fig. 9 shows a comparison for the vacuum point versus the background packing fraction η_0 for $\rho_- = 1.0$. This comparison is for the value of η_+ at which the vacuum point first occurs, that is the value of ρ_+ at which $|u|$ first vanishes within the DSW, as discussed in Section 8. The full modulation theory gives that this vacuum point is given implicitly by (75), while higher order NLS equation modulation theory gives that it is the solution of (77), with the NLS equation modulation theory value given by this expression with $\alpha = 0$. The NLS equation modulation theory gives a constant vacuum point independent of η_0, in contrast to the other modulation theories. The full modulation theory gives near perfect agreement for the vacuum point for the full range of background packing fractions η_0, with the overall difference from the numerical value less than 0.1%. The higher order NLS modulation theory gives reasonable agreement, with increasing disagreement as the background packing fraction decreases, similar to the amplitude comparison of Fig. 6. The difference grows to 2.8% at $\eta_0 = 0.01$. This is due to the higher order NLS equation (8) being valid in the limit $|\eta - \eta_0| \ll 1$, which becomes less valid as η_0 decreases. As for the other DSW properties discussed above, the NLS equation modulation theory does not give good agreement for the vacuum point, again highlighting the importance of the higher order terms in the constitutive law (2) for the colloid.

10. Conclusions

The DSW solution for optical beam propagation in a defocusing colloidal solution has been derived. As the full Whitham modulation theory [1,25,26] is not available, due to the underlying colloid

Please cite this article in press as: X. An, et al., Optical dispersive shock waves in defocusing colloidal media, Physica D (2016), http://dx.doi.org/10.1016/j.physd.2016.11.004

equations (1) and (2) not being integrable [32], modulation equations for the leading and trailing edges of the DSW were derived using the method of El [4,33,34]. This method enables the derivation of differential equations for these leading and trailing edges without knowledge of the full modulation equations by using the degenerate nature of these modulation equations at the edges of the DSW for cases in which the DSW is of KdV type. It was found that in the limit of low beam power, or small deviations of the colloid concentration from the background value, the full colloid equations can be approximated by a higher order NLS equation. El's method was also used to derive the leading and trailing edges of DSW for this higher order NLS equation, as has been done in previous work [18,36].

The modulation theory for the full colloid equations was found to give near perfect predictions for the amplitude and velocity of the trailing solitary wave of the DSW and the velocity of the linear, leading edge of the DSW. It was also found that the modulation theory for the higher order NLS equation gave reasonable predictions for the leading and trailing edges of the DSW, but not for other properties, such as the vacuum point. This highlights that the full constitutive law (2) is not always necessary and that Taylor expansions of it for small packing fractions can lead to adequate approximations to the full constitutive law. The constitutive law (2) is one of many derived under various approximations for colloidal media. It is an open question as to whether these full constitutive laws are needed and whether low power Taylor expansions provide adequate approximations. However, the present work highlights the power of El's method to derive the leading and trailing edges of a KdV-like DSW, particularly for nonlinear wave equations which are not integrable. One extension of this work is to optical colloidal media with a more general constitutive relation $g(\eta)$ [42]. Hopefully, this theoretical and numerical study will motivate some future experimental studies of dark DSWs in colloidal and other optical media.

Acknowledgements

The authors would like to thank the two anonymous reviewers for their helpful comments.

Appendix. Amplitude–velocity relation for the grey colloidal solitary wave

In this appendix, the amplitude–velocity relation for a grey colloidal solitary wave is derived. Let us seek a grey solitary wave solution of the colloid equations (1) and (2) of the form

$$u = f(\theta)e^{-i\sigma z}, \qquad \eta = \eta(x - Vz), \qquad \theta = x - Vz, \tag{A.1}$$

where V is the velocity and σ is the propagation constant. The carrier wave giving the level as $\theta \to \pm\infty$ is

$$u = u_\infty e^{-i\sigma z}, \qquad \sigma = \eta_\infty - \eta_0, \qquad g(\eta_\infty) - g_0 = u_\infty^2. \tag{A.2}$$

Substituting the grey solitary wave form (A.1) into the colloid equations (1) and (2) gives

$$\sigma f - iVf' + \frac{1}{2}f'' - (\eta - \eta_0)f = 0, \qquad |f|^2 = g(\eta) - g_0. \tag{A.3}$$

We split this equation into real and imaginary parts with $f = f_r + if_i$, giving

$$\sigma f_r + Vf_i' + \frac{1}{2}f_r'' - (\eta - \eta_0)f_r = 0, \tag{A.4}$$

$$\sigma f_i - Vf_r' + \frac{1}{2}f_i'' - (\eta - \eta_0)f_i = 0 \tag{A.5}$$

and σ given by (A.2). Multiplying the real part (A.4) by f_r' and the imaginary part (A.5) by f_i', adding and then integrating once gives

$$\frac{1}{2}\sigma\left(f_r^2 + f_i^2\right) + \frac{1}{4}\left(f_r'^2 + f_i'^2\right) - \int (\eta - \eta_0)\left(f_r f_r' + f_i f_i'\right) d\theta = D, \tag{A.6}$$

where D is a constant of integration. Differentiating the constitutive law (A.3) enables the integral to be rearranged as an integral in η, so that (A.6) can be determined explicitly as

$$\sigma\left(f_r^2 + f_i^2\right) + \frac{1}{2}\left(f_r'^2 + f_i'^2\right) - F(\eta, \eta_\infty) = D, \tag{A.7}$$

with

$$F(\eta, \eta_\infty) = \left[\frac{1}{(1-\eta)^3} - \frac{1}{(1-\eta)^2} - \frac{1}{1-\eta} + \frac{\eta}{2} - \frac{\eta_0}{2}g(\eta)\right]_{\eta_\infty}^{\eta}. \tag{A.8}$$

The constant of integration D can be found by taking $\theta \to \infty$, resulting in $D = \sigma u_\infty^2$, since $|f|^2 \to u_\infty^2$ as $\theta \to \infty$.

Similarly, multiplying the real part (A.4) by f_i and the imaginary part (A.5) by f_r, subtracting and integrating gives

$$f_i f_r' - f_r f_i' = \left(u_\infty^2 - f_r^2 - f_i^2\right)V. \tag{A.9}$$

Let us now consider the minimum of the grey solitary wave profile $|u|$ and denote values at this minimum by an m subscript. At the minimum for $|u|^2$, we have that

$$f_{rm}f_{rm}' + f_{im}f_{im}' = 0. \tag{A.10}$$

Hence, the imaginary part expression (A.9) gives

$$V = \frac{|f_m|^2}{f_{im}\left(u_\infty^2 - |f_m|^2\right)}f_{rm}'. \tag{A.11}$$

Similarly, using the minimum relation (A.10) in the real part expression (A.8) we have

$$\frac{|f_m|^2}{f_{im}^2}(f_{rm}')^2 = 2D - 2\sigma|f_m|^2 + 2F(\eta_m, \eta_\infty), \tag{A.12}$$

where $F(\eta_m, \eta_\infty)$ is similarly defined as $F(\eta, \eta_\infty)$. Combining (A.11) and (A.12) we can deduce the amplitude–velocity relation for a grey colloid solitary wave as

$$V = \frac{\sqrt{2}|f_m|\sqrt{\sigma u_\infty^2 - \sigma|f_m|^2 + F(\eta_m, \eta_\infty)}}{u_\infty^2 - |f_m|^2}. \tag{A.13}$$

We note that this amplitude–velocity relation has been derived independently of the solution for the grey solitary wave.

References

[1] G. Whitham, Linear and Nonlinear Waves, Wiley and Sons, New York, 1974.
[2] N. Zabusky, M. Kruskal, Interaction of solitons' in a collisionless plasma and the recurrence of initial states, Phys. Rev. Lett. 15 (1965) 240–243.
[3] A. Newell, Solitons in Mathematics and Physics, SIAM, Philadelphia, 1985.
[4] G. El, M. Hoefer, Dispersive shock waves and modulation theory, Physica D 333 (2016) 11–65.
[5] T. Benjamin, M. Lighthill, On cnoidal waves and bores, Proc. R. Soc. Lond. Ser. A 224 (1954) 448–460.
[6] R. Johnson, A non-linear equation incorporating damping and dispersion, J. Fluid Mech. 42 (1970) 49–60.
[7] R. Clarke, R. Smith, D. Reid, The morning glory of the Gulf of Carpentaria: an atmospheric undular bore, Mon. Weather Rev. 109 (1981) 1725–1750.
[8] D. Christie, Long nonlinear waves in the lower atmosphere, J. Atmos. Sci. 46 (1989) 1989.

Please cite this article in press as: X. An, et al., Optical dispersive shock waves in defocusing colloidal media, Physica D (2016), http://dx.doi.org/10.1016/j.physd.2016.11.004

[9] A. Porter, N. Smyth, Modelling the morning glory of the gulf of carpentaria, J. Fluid Mech. 454 (2002) 1–20.
[10] N. Smyth, P. Holloway, Hydraulic jump and undular bore formation on a shelf break, J. Phys. Oceanogr. 18 (1988) 947–962.
[11] J. Esler, J. Pearce, Dispersive dam-break and lock-exchange flows in a two-layer fluid, J. Fluid Mech. 667 (2011) 555–585.
[12] D. Scott, D. Stevenson, Magma solitons, Geophys. Res. Lett. 11 (1984) 1161–1164.
[13] T. Marchant, N. Smyth, Approximate solutions for magmon propagation from a reservoir, IMA J. Appl. Math. 70 (2005) 796–813.
[14] N. Lowman, M. Hoefer, Dispersive shock waves in viscously deformable media, J. Fluid Mech. 718 (2013) 524–557.
[15] N. Lowman, M. Hoefer, Fermionic shock waves: Distinguishing dissipative versus dispersive resolutions, Phys. Rev. A 88 (2013) 013605.
[16] G. El, A. Kamchatnov, V. Khodorovskii, E. Annibale, A. Gammal, Two-dimensional supersonic nonlinear Schrödinger flow past an extended obstacle, Phys. Rev. E 80 (2009) 046317.
[17] C. Barsi, W. Wan, C. Sun, J. Fleischer, Dispersive shock waves with nonlocal nonlinearity, Opt. Lett. 32 (2007) 2930–2932.
[18] G. El, A. Gammal, E. Khamis, R. Kraenkel, A. Kamchatnov, Theory of optical dispersive shock waves in photorefractive media, Phys. Rev. A 76 (2007) 053813.
[19] W. Wan, S. Jia, J. Fleischer, Dispersive superfluid-like shock waves in nonlinear optics, Nat. Phys. 3 (2007) 46–51.
[20] M. Conforti, F. Baronio, S. Trillo, Resonant radiation shed by dispersive shock waves, Phys. Rev. A 89 (2014) 013807.
[21] M. Conforti, S. Trillo, Radiative effects driven by shock waves in cavity-less four-wave mixing combs, Opt. Lett. 39 (2014) 5760–5763.
[22] S. Malaguti, M. Conforti, S. Trillo, Dispersive radiation induced by shock waves in passive resonators, Opt. Lett. 39 (2014) 5626–5629.
[23] N. Ghofraniha, C. Conti, G. Ruocco, S. Trillo, Shocks in nonlocal media, Phys. Rev. Lett. 99 (2007) 043903.
[24] J. Wang, J. Li, D. Lu, Q. Guo, W. Hu, Observation of surface dispersive shock waves in a self-defocusing medium, Phys. Rev. A 91 (2015) 063819.
[25] G. Whitham, A general approach to linear and non-linear dispersive wave using a lagrangian, J. Fluid Mech. 22 (1965) 273–283.
[26] G. Whitham, Non-linear dispersive waves, Proc. R. Soc. Lond. Ser. A 283 (1965) 238–261.
[27] A. Gurevich, L. Pitaevskii, Nonstationary structure of a collision-less shock wave, Sov. Phys.—JETP 33 (1974) 291–297.
[28] B. Fornberg, G. Whitham, Numerical and theoretical study of certain non-linear wave phenomena, Philos. Trans. R. Soc. Lond. Ser. A 289 (1978) 373–404.
[29] G. El, V. Geogjaev, A. Gurevich, A. Krylov, Decay of an initial discontinuity in the defocusing NLS hydrodynamics, Physica D 87 (1995) 186–192.
[30] A. Minzoni, N. Smyth, A modulation solutions of the signalling problem for the equation of self-induced transparency in the Sine-Gordon limit, Methods Appl. Anal. 4 (1997) 1–10.
[31] A. Kamchatnov, Y.-H. Kuo, T.-C. Lin, T.-L. Horng, S.-C. Gou, R. Clift, G. El, R. Grimshaw, Undular bore theory for the Gardner equation, Phys. Rev. E 86 (2012) 036605.
[32] H. Flaschka, M. Forest, D. McLaughlin, Multiphase averaging and the inverse spectral solution of the korteweg-de vries equation, Comm. Pure Appl. Math. 33 (1980) 739–784.
[33] G. El, V. Khodorovskii, A. Tyurina, Determination of boundaries of unsteady oscillatory zone in asymptotic solutions of non-integrable dispersive wave equations, Phys. Lett. A 318 (2003) 526–536.
[34] G. El, Resolution of a shock in hyperbolic systems modified by weak dispersion, Chaos 15 (2005) 037103.
[35] N. Smyth, Dispersive shock waves in nematic liquid crystals, Physica D 333 (2016) 301–309.
[36] M. Crosta, S. Trillo, A. Fratalocchi, The Whitham approach to dispersive shocks in systems with cubic-quintic nonlinearities, New J. Phys. 14 (2012) 093019.
[37] W. Wan, D. Dylov, C. Barsi, J. Fleischer, Diffraction from an edge on a self-defocusing medium, Opt. Lett. 35 (2010) 2819–2821.
[38] M. Matuszewski, W. Krolikowski, Y. Kivshar, Spatial solitons and light-induced instabilities in colloidal media, Opt. Express 16 (2008) 1371–1376.
[39] M. Matuszewski, W. Krolikowski, Y. Kivshar, Soliton interactions and transformations in colloidal media, Phys. Rev. A 79 (2009) 023814.
[40] D. Talapin, A. Rogach, M. Haase, H. Welle, Evolution of an ensemble of nanoparticles in a colloidal solution: theoretical study, J. Phys. Chem. B 105 (2001) 12278–12285.
[41] S. Fardad, A. Bezryadina, P. Zhang, Z. Chen, D. Christodoulides, Tunable polarizability and self-trapping of light in colloidal suspensions of gold nanoparticles, CLEO: 2013, OSA Technical Digest (online) (Optical Society of America, 2013) (2013) QM3E.8.
[42] A. Azmi, T. Marchant, Dispersive shock waves in colloids with temperature dependent compressibility, J. Nonlinear Opt. Phys. 23 (2014) 1450043.
[43] T. Marchant, N. Smyth, Semi-analytical solutions for dispersive shock waves in colloidal media, J. Phys. B: At. Mol. Opt. Phys. 45 (2012) 145401.
[44] T. Marchant, N. Smyth, Approximate techniques for dispersive shock waves in nonlinear media, J. Nonlinear Opt. Phys. 21 (2012) 1250035.
[45] Y. Kivshar, Optical Solitons: From Fibers to Photonic Crystals, Academic Press, San Diego, 2003.
[46] M. Ablowitz, A. Demirci, Y.-P. Ma, Dispersive shock waves in the Kadomtsev–Petviashvili and two-dimensional Benjamin–Ono equations, Physica D 333 (2016) 84–98.
[47] K. Khusnutdinova, X. Zhang, Nonlinear ring waves in a two-layer fluid, Physica D 333 (2016) 208–211.
[48] R. El-Ganainy, D. Christodoulides, C. Rotschild, M. Segev, Soliton dynamics and self-induced transparency in nonlinear nanosuspensions, Opt. Express 15 (2007) 10207.
[49] J. Hansen, I. McDonald, Theory of Simple Liquids, Academic Press, London, 1979.
[50] M. Hoefer, Shock waves in dispersive Eulerian fluids, J. Nonlinear Sci. 24 (2014) 525–577.
[51] G. El, N. Smyth, Radiating dispersive shock waves in non-local optical media, Proc. R. Soc. Lond. Ser. A 472 (2016) 20150633.
[52] T. Grava, C. Klein, Numerical solution of the small dispersion limit of the Korteweg-de Vries equation and Whitham equations, Comm. Pure Appl. Math. 60 (2007) 1623–1664.
[53] T. Grava, C. Klein, A numerical study of the small dispersion limit of the Korteweg-de Vries equation and asymptotic solutions, Physica D 241 (2012) 2246–2264.
[54] J. Leach, D. Needham, The large-time development of the solution to an initial-value problem for the Korteweg-de Vries equation: I initial data has a discontinuous expansive step, Nonlinearity 21 (2008) 2391–2408.

Please cite this article in press as: X. An, et al., Optical dispersive shock waves in defocusing colloidal media, Physica D (2016), http://dx.doi.org/10.1016/j.physd.2016.11.004